



OPEN ACCESS

EDITED BY

Jiaxiang Chen,
Mayo Clinic, United States

REVIEWED BY

Yan Yang,
The First Affiliated Hospital of Bengbu
Medical College, China
Xiaohui Zhu,
Shenzhen Technology University, China

*CORRESPONDENCE

Wei Gao

✉ gaoweisxent@sxent.org
Changming An

✉ anchangming@cicams.ac.cn
Yongyan Wu

✉ wuyongyan@sxent.org

†These authors have contributed equally to
this work

RECEIVED 08 December 2022

ACCEPTED 11 April 2023

PUBLISHED 02 May 2023

CITATION

Zheng X, Gao W, Zhang Z, Xue X, Mijiti M,
Guo Q, Wusiman D, Wang K, Zeng X,
Xue L, Guo Z, An C and Wu Y (2023)
Identification of a seven-lncRNAs panel
that serves as a prognosis predictor and
contributes to the malignant progression
of laryngeal squamous cell carcinoma.
Front. Oncol. 13:1106249.
doi: 10.3389/fonc.2023.1106249

COPYRIGHT

© 2023 Zheng, Gao, Zhang, Xue, Mijiti, Guo,
Wusiman, Wang, Zeng, Xue, Guo, An and
Wu. This is an open-access article distributed
under the terms of the [Creative Commons
Attribution License \(CC BY\)](#). The use,
distribution or reproduction in other
forums is permitted, provided the original
author(s) and the copyright owner(s) are
credited and that the original publication in
this journal is cited, in accordance with
accepted academic practice. No use,
distribution or reproduction is permitted
which does not comply with these terms.

Identification of a seven-lncRNAs panel that serves as a prognosis predictor and contributes to the malignant progression of laryngeal squamous cell carcinoma

Xiwang Zheng^{1,2†}, Wei Gao^{1,3,4*†}, Zhe Zhang^{1,5†}, Xuting Xue^{1,2†},
Maierhaba Mijiti¹, Qingbo Guo¹, Dilinaer Wusiman⁶, Kai Wang⁷,
Xianhai Zeng^{3,4}, Lingbin Xue^{3,4}, Zekun Guo⁸,
Changming An^{1,6*} and Yongyan Wu^{1,3,4*}

¹Shanxi Key Laboratory of Otorhinolaryngology Head and Neck Cancer, First Hospital of Shanxi Medical University, Taiyuan, Shanxi, China, ²Shanxi Province Clinical Medical Research Center for Precision Medicine of Head and Neck Cancer, First Hospital of Shanxi Medical University, Taiyuan, Shanxi, China, ³Department of Otolaryngology Head & Neck Surgery, Longgang Otolaryngology Hospital, Shenzhen, Guangdong, China, ⁴Shenzhen Institute of Otolaryngology & Key Laboratory of Otolaryngology, Longgang Otolaryngology Hospital, Shenzhen, Guangdong, China, ⁵Shenzhen Eye Hospital, Jinan University, Shenzhen Eye Institute, Shenzhen, Guangdong, China, ⁶Department of Head and Neck Surgery, National Cancer Center/National Clinical Research Center for Cancer/Cancer Hospital, Chinese Academy of Medical Sciences and Peking Union Medical College, Beijing, China, ⁷Department of Otolaryngology Head & Neck Surgery, Southern University of Science and Technology Hospital, Southern University of Science and Technology, Shenzhen, Guangdong, China, ⁸College of Life Sciences, Northwest A&F University, Yangling, Shaanxi, China

Background: Laryngeal squamous cell carcinoma (LSCC) is one of the most frequent head and neck cancers worldwide. Long non-coding RNAs (lncRNAs) play a critical role in tumorigenesis. However, the clinical significance of lncRNAs in LSCC remains largely unknown.

Methods: In this study, transcriptome sequencing was performed on 107 LSCC and paired adjacent normal mucosa (ANM) tissues. Furthermore, RNA expression and clinical data of 111 LSCC samples were obtained from The Cancer Genome Atlas (TCGA) database. Bioinformatics analysis were performed to construct a model for predicting the overall survival (OS) of LSCC patients. Moreover, we investigated the roles of lncRNAs in LSCC cells through loss-of-function experiments.

Results: A seven-lncRNAs panel including ENSG00000233397, BARX1-DT, LSAMP-AS1, HOXB-AS4, MNX1-AS1, LINC01385, and LINC02893 was identified. The Kaplan–Meier analysis demonstrated that the seven-lncRNAs panel was significantly associated with OS (HR:6.21 [3.27–11.81], p-value<0.0001), disease-specific survival (DSS) (HR:4.34 [1.83–10.26], p-value=0.0008), and progression-free interval (PFI) (HR:3.78 [1.92–7.43], p-value=0.0001). ROC curves showed the seven-lncRNAs panel predicts OS with

good specificity and sensitivity. Separately silencing the seven lncRNAs inhibited the proliferation, migration, and invasion capacity of LSCC cells.

Conclusion: Collectively, this seven-lncRNAs panel is a promising signature for predicting the prognosis of LSCC patients, and these lncRNAs could serve as potential targets for LSCC treatment.

KEYWORDS

laryngeal squamous cell carcinoma, biomarker, long non-coding RNA, oncogene, prognosis

Introduction

Laryngeal squamous cell carcinoma (LSCC) is the second most frequent malignancy of the head and neck, or the upper respiratory tract (1, 2). Despite the improvements in curative techniques, laryngeal cancer is still one of the few cancers in which the 5-year survival rate continues to decline, over the past 40 years (3, 4). LSCC has the malignant characteristics of local invasion and cervical lymph node metastasis, which are major risk factors of mortality for LSCC patients (5, 6). Consequently, about 60% of LSCC patients have already progressed to the advanced clinical stages (III/IV) at diagnosis, and thus missed the optimal therapeutic window (7).

Molecular biomarkers or signatures are extremely valuable tools for the early diagnosis and accurate prognosis of cancer in modern times (8, 9). Long non-coding RNAs (lncRNAs) are a class of non-protein coding RNA molecules with more than 200 nucleotides (10) that have a variety of regulatory functions on cancer cell proliferation, genomic stability, metabolism, angiogenesis, immunity, and metastasis (11–16). Moreover, lncRNAs were considered important candidate biomarkers due to their specific spatiotemporal expression and diversity in cancer (17). Multiple studies reported that a variety of lncRNAs were identified as promising biomarkers for the diagnosis and prognosis of cancers (18–20), and some of these are already being used in clinical trials (21, 22). Furthermore, it has been shown that lncRNAs are involved in regulating the progression of LSCC, and may therefore be used as potential disease biomarkers (23, 24). Unfortunately, there are currently no molecular biomarkers or signatures used for the diagnosis and prognosis of LSCC. Hence, it is necessary to explore more putative lncRNA biomarkers or signatures with high specificity and sensitivity for LSCC.

High-throughput RNA sequencing (RNA-Seq) provides an efficient approach for the identification of differentially expressed genes in large-scale samples. In this study, RNA-Seq was performed to screen for differentially expressed lncRNAs in 107 LSCC and paired adjacent normal mucosa (ANM) tissues (Shanxi cohort). Furthermore, the lncRNAs expression and clinical data of 111 LSCC and 12 normal samples were obtained from The Cancer Genome Atlas (TCGA) database. By integrating the Shanxi cohort and the TCGA cohort data, we investigated the lncRNA expression

profiles, determined the pathways involved with dysregulated lncRNAs, and identified lncRNAs associated with the survival of LSCC patients. We constructed a seven-lncRNAs signature with high specificity and sensitivity and developed a nomogram for predicting the prognosis of LSCC patients. Lastly, we explored the functional roles of the seven lncRNAs in LSCC cells. Our findings provide novel potential biomarkers and molecular targets for the prognosis evaluation and therapy of LSCC.

Materials and methods

Tissue samples

LSCC tissues and paired ANM tissues were collected from patients who had undergone surgery at the Department of Otolaryngology Head and Neck Surgery, First Hospital of Shanxi Medical University. None of the patients received chemotherapy or radiotherapy before surgery. The clinical samples were collected from LSCC patients after obtaining their informed consent. Studies were performed with the approval of the medical ethics committee of First Hospital of Shanxi Medical University.

RNA isolation, library preparation, and RNA-sequencing

Total RNA was isolated using TRIzol reagent (Ambion, USA) following the manufacturer's protocol. After evaluation of purity, concentration, and integrity, 3 µg of RNA per sample was used in library preparation for RNA sequencing. The rRNA was removed using the Ribo-zero rRNA Removal Kit (Epicentre, USA), and the rRNA-depleted sample was subsequently used to generate sequencing libraries using the NEB Next Ultra Directional RNA Library Prep Kit for Illumina (NEB, USA) according to the manufacturer's protocols. In brief, the rRNA-depleted RNA samples were subjected to RNA fragmentation, first strand cDNA synthesis with random hexamer primers, second strand cDNA synthesis with dUTP, adenylation of 3' ends, barcoded adapter

ligation, purification, and amplification using PCR to generate sequencing libraries. After cluster generation, libraries were sequenced on an Illumina HiSeq 4000 platform by Novogene (Beijing, China).

Analysis of RNA-sequencing data

Clean reads were obtained by removing reads adapter, reads containing poly-N, and low-quality reads from raw data. The reads mapping and transcript assembly was done using TopHat (v2.0.9) and Cufflinks (v2.1.1) based on the human reference genome (GRCh37) from the Ensembl database (<https://www.ensembl.org/>). Then, the coding potential of transcripts was predicted using CPC2 (beta) and CNCI (v2). Finally, the read counts in fragments per kilobase million (FPKM) of transcripts were used as input data for a more in-depth bioinformatic analysis. The TCGA expression data of LSCC were obtained from the TCGA data portal (<https://cancergenome.nih.gov/>). The associated clinical features were obtained from the University of California, Santa Cruz Xena (UCSC Xena; <https://xenabrowser.net/>) database. The significantly differentially expressed lncRNAs in the Shanxi and TCGA cohorts were screened using the R package DEseq2 (v1.26.0) (25) with the cut-off $p\text{-value} < 0.05$ and $|\log_2(\text{Fold change})| \geq 1$.

Unsupervised learning analysis

Complete-linkage clustering, which is one of the hierarchical clustering algorithms, was used to analyze the differential expression of lncRNAs in relation to various clinical features. The heat map to visualize the expression data was constructed using the R package pheatmap (v1.0.12, <https://CRAN.R-project.org/package=pheatmap>). Principal component analysis (PCA) was used to reduce the dimensionality of high dimensional expression datasets and evaluate the degree of difference between LSCC and normal tissue. The 3D visualization of PCA was realized using the R package pca3d (v0.10.1, <https://CRAN.R-project.org/package=pca3d>).

Gene set enrichment analysis

Functional annotation of dysregulated lncRNAs in LSCC was performed using the GSEA (v3.0) software with Molecular Signatures Database (v7.0, <https://www.gsea-msigdb.org/gsea/msigdb/>). Significantly upregulated and downregulated lncRNAs in both the Shanxi and TCGA cohorts were obtained by Venn analysis. Pearson correlation analysis with Student's *t*-test was used to obtain protein-coding RNAs that are correlated with lncRNAs based on their expression levels, with a cut-off set at $|\text{Pearson's } r| \geq 0.4$ and $p\text{-value} < 0.05$. Based on the ranking of Pearson's *r*, the five most positively and five most negatively correlated protein-coding RNAs to each of the lncRNAs were selected as the input data for GSEA. Mutual functional pathways in two LSCC cohorts were mined using a cut-off set at FDR $q\text{-value} \leq 0.01$ after GSEA.

Prediction of the biological processes and pathways associated with the identified seven lncRNAs

The previously identified protein-coding RNAs that were correlated with the expression of the seven lncRNAs were used to determine the different associated biological signaling pathways using Metascape (<https://metascape.org/>).

Survival analysis

Univariate Cox proportional hazards regression analysis was used to investigate the relationship between the continuous expression levels of each significantly dysregulated lncRNA and the overall survival (OS) of patients in the TCGA cohort. A total of 111 LSCC patients' data from TCGA database were used for survival analysis, in which 50 patients were reached the survival endpoint. Based on the expression fold-change of each lncRNA, the output of the Cox regression analysis was divided into an upregulation set and a downregulation set. Under the criterion of $p\text{-value} < 0.05$, 20 lncRNAs in the upregulation set and 4 lncRNAs in the downregulation set were defined as significant high-risk lncRNAs for LSCC patients. The least absolute shrinkage and selection operator (LASSO) algorithm with a penalty parameter of 1000 and a 10-fold cross-validation was used to shrink sparse high-dimensional data and develop a prognostic prediction model from the output of the Cox regression analysis. The LASSO algorithm was implemented using the R package glmnet (v2.0.16, <https://CRAN.R-project.org/package=glmnet>). To determine the risk levels of the prognostic prediction model for OS, the risk score for each LSCC patient was calculated using the formula: $\text{risk score} = \sum_{i=1}^n (c_{lncRNAi} \times e_{lncRNAi})$; where $c_{lncRNAi}$ is the relation coefficient of the risk factor *lncRNAi*; $e_{lncRNAi}$ is the expressional value of the risk factor *lncRNAi*; and *n* is the number of lncRNAs included in the prognostic prediction model. The LSCC patients were classified into high or low risk groups according to the median value of the computed risk scores. The Kaplan-Meier (K-M) estimator model with the log-rank test was used to estimate the OS, disease-specific survival (DSS), and progression-free interval (PFI) for LSCC patients between the high and low risk groups. The survival curve was realized using the R packages survival (v2.44-1.1, <https://cran.r-project.org/package=survival>) and survminer (v0.4.4, <https://CRAN.R-project.org/package=survminer>). The sensitivity and specificity of the lncRNAs prognostic prediction model were analyzed using a time-dependent receiver operating characteristic (ROC) curve. The area under the curve (AUC) was compared among the 1-, 3- and 5-year survival rates. The calculation and visualization of the ROC curves were done using the R package timeROC (v0.3, <https://CRAN.R-project.org/package=timeROC>). Moreover, a total of 86 LSCC samples with follow-up data was used to validate the efficiency of prognostic model. The expression levels of 7 lncRNAs in the 86 LSCC samples were determined by qPCR analysis. A nomogram for predicting OS was built using the R package rms (v5.1-3, <https://CRAN.R-project.org/package=rms>).

The survival probabilities were predicted for the 1-, 3- and 5-year marks. The validation of the nomogram prediction model was accessed using bootstrapped calibration curves.

Construction of the lncRNAs-miRNAs-mRNAs network

The correlation among seven lncRNAs was analyzed using the R package *stats* (v4.1.0) and visualized using the R package *corrplot* (v 0.92, <https://cran.r-project.org/package=corrplot>). An lncRNAs-miRNAs-mRNAs network was constructed based on competitive endogenous RNA (ceRNAs). For target miRNA prediction of seven lncRNAs, miRanda (v3.3a, <https://anaconda.org/bioconda/miranda>), LncTar (v1.0, <http://www.cuilab.cn/lncstar>) and RNA22 (v2.0, <https://cm.jefferson.edu/rna22/>) were used to independently predict the binding between lncRNAs and miRNAs. Next, the top 30 miRNAs with strongest binding ability to each lncRNA in three softwares were intersected to obtain potential target miRNAs. For target mRNA prediction of miRNAs, Targetscan (v7.1, <https://www.targetscan.org/>), miRdb (<https://mirdb.org/mirdb/>) and miRWalk (<http://mirwalk.umm.uni-heidelberg.de/>) were utilized. Target Score ≥ 20 in miRDB, energy ≤ -5 in miRWalk and Total context++ score ≤ -0.1 in Targetscan were used as the threshold, and target mRNAs for each miRNA were obtained from intersection of three databases. Finally, Cytoscape (v3.7.1, <https://cytoscape.org/>) was used to construct the lncRNAs-miRNAs-mRNAs network.

Cell culture, transfection, and quantitative real-time PCR

Human LSCC TU-177 cell lines (Bioleaf Biotech, China) were cultured in Dulbecco's Modified Eagle's Medium (DMEM; Life Technologies, USA) supplemented with 10% fetal bovine serum (FBS; BI, USA). Human LSCC FD-LSC-1 (26) cell lines were cultured with Bronchial Epithelial Cell Growth Medium (BEGM; Lonza, Switzerland) supplemented with 10% FBS. All cells were maintained in a humid atmosphere of 5% CO₂ at 37°C. The siRNAs used to target lncRNAs were synthesized by GenePharma Co., Ltd (Shanghai China). The siRNA sequences are listed in Table S1. Cells (2.0×10^5 cells per well) were seeded in 6-well plates 24 h before transfection. The siRNAs were transfected using Lipofectamine 3000 (ThermoFisher Scientific, USA) according to the manufacturer's protocol. A qPCR analysis was performed to determine the relative expression levels of the target lncRNAs. Expression levels of 18S rRNA were used as internal controls. The primer sequences used are listed in Table S2.

Cell proliferation, migration, and invasion assays

Cell proliferation was assessed using the EdU staining kit (RiboBio, Guangzhou, China) according to the manufacturer's

protocol. Trans-well migration and invasion assays were performed as previously described with modification (27). Briefly, for the migration assay, cells were seeded in 24-well trans-well plates (Falcon, USA) with a density of 1×10^6 cells per well in 100 μ L of serum-free media. Meanwhile, for the invasion assay, 1×10^5 cells were seeded in each well of the 24-well trans-well plates coated with Matrigel (Corning, USA). After 24 h of incubation, the cells in the upper chamber of the membranes were removed using cotton swabs, then cells in the lower chamber were stained with crystal violet (Amresco, USA) for 10 min and washed with PBS.

Results

Determining the lncRNA expression profile of LSCC patients by RNA-seq

A total of 107 LSCC and paired ANM tissues were collected from 107 patients who were clinically diagnosed with LSCC to constitute the Shanxi cohort. The RNA samples from the Shanxi cohort were subjected to transcriptome sequencing (Figure 1A). Furthermore, the RNA-seq data of 111 LSCC patients were obtained from the TCGA database. The analysis workflow used in this study is shown in Figure S1. The PCA results showed that the lncRNA expression patterns in LSCC tissues are different from that of the paired ANM tissues (Figure 1B). This trend was further confirmed by the TCGA cohort (Figure 1C). Next, an unsupervised hierarchical clustering based on the lncRNA expression data and clinical features was performed. The results showed that numerous lncRNAs were differentially expressed between the LSCC and ANM/normal groups (Figures 1D, E).

Dysregulated lncRNAs in LSCC are involved in tumorigenesis-related processes and pathways

Based on a threshold of $p < 0.05$ and $|\text{fold-change}| \geq 2$, a total of 6,060 differentially expressed lncRNAs were identified in the Shanxi cohort. Out of these, 2,949 were upregulated and 3,111 were downregulated in LSCC tissues compared with ANM tissues (Figure 2A and Table S3). Meanwhile, in the TCGA cohort, 4,381 upregulated and 1,524 downregulated lncRNAs were identified in LSCC samples compared to normal samples (Figure 2B and Table S4). Using Venn analysis, we obtained 594 upregulated and 197 downregulated lncRNAs from both cohorts (Figure 2C), which were named as significantly dysregulated lncRNAs (SDLs). Next, we predicted the biological processes and pathways associated with the SDLs using GSEA. Results showed 36 mutual biological processes and pathways (FDR q-value ≤ 0.01) in both cohorts, including terms such as epithelial to mesenchymal transition (EMT), nasopharyngeal carcinoma, cell cycle checkpoints, tumorigenesis, thyroid carcinoma poorly differentiated, and malignant mesothelioma (Figure 2D). These suggested that the SDLs were involved in the regulation of multiple tumorigenesis-related processes and pathways.

EMT plays an important role in the development and metastasis of cancer (28, 29). We observed that the SDLs in both LSCC cohorts were significantly enriched in EMT (Figures 2E, F), suggesting that the dysregulated lncRNAs may affect LSCC invasion and metastasis by regulating the EMT process.

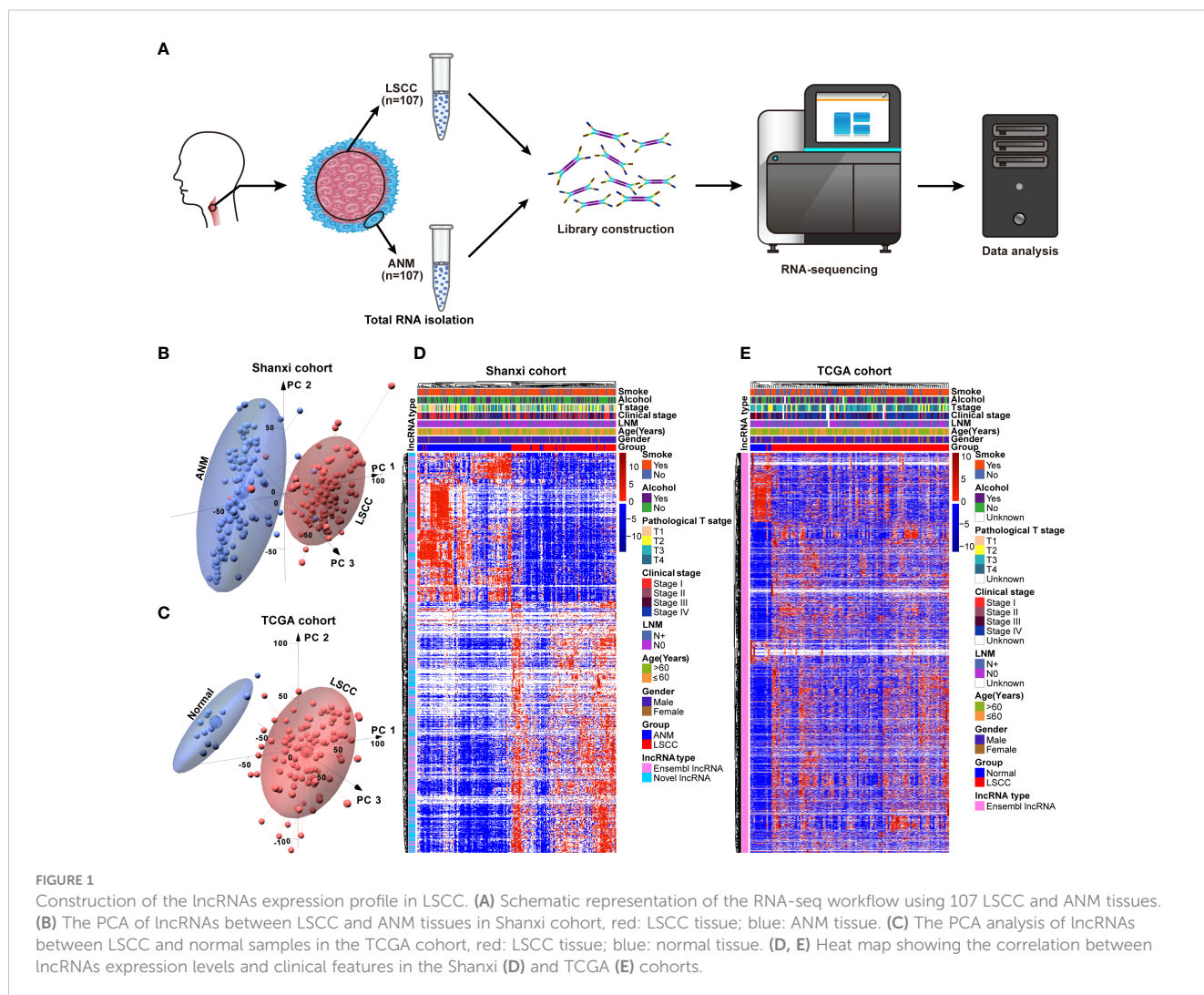
Screening for lncRNAs associated with the OS of LSCC patients

To screen for lncRNAs that are significantly associated with the OS of LSCC patients, all SDLs and prognosis-related clinical information of TCGA patients were subjected to Cox proportional hazards regression analysis. Using the criterion of p -value ≤ 0.05 , 20 upregulated (TEX41, LINC00392, LINC02575, ENSG00000233397 (named as ENSG233397 thereafter), BARX1-DT, TSPEAR-AS1, ENSG00000236841, LSAMP-AS1, HOXB-AS4, MNX1-AS1, LINC01391, LINC02086, LINC02315, LINC01385, ENSG00000253477, CABP1-DT, ENSG00000260978, ENSG00000267919, LINC02893 (also known as AL513318.2), and ENSG00000272763) and 4 downregulated (LINC00278, HOXA-

AS2, LINC02568, and LINC02188) lncRNAs were obtained from the univariate Cox analysis (Figures 3A, B). The association between the expression levels of these 24 lncRNAs and OS of LSCC patients was verified using K-M survival analysis (Figures S2, S3). Results showed that LSCC patients with high expression levels (\geq median FPKM) of each of the 20 upregulated lncRNAs had a shorter median OS time than that of the low expression group ($<$ median FPKM). In contrast, LSCC patients with high expression levels of each of the 4 downregulated lncRNAs had a longer median OS time than that of the low expression group (Figure 3C).

Construction and validation of a seven-lncRNAs panel for predicting the prognosis of LSCC patients

To construct a model for predicting the prognosis of LSCC patients, LASSO regression analysis was used to narrow down the candidate lncRNAs based on the output of the Cox analysis. This led to the identification of seven lncRNAs including ENSG233397, BARX1-DT, LSAMP-AS1, HOXB-AS4, MNX1-



AS1, LINC01385, and LINC02893 (Figure 4A). These seven lncRNAs were significantly upregulated in LSCC tissues compared to normal counterparts in both the Shanxi and TCGA cohorts (Figures S4, S5). Combining the relative expression of the lncRNAs and their corresponding coefficients, the risk score for the seven-lncRNAs of each patient was calculated as follows: risk score = $0.1331 \times e_{ENSG233397} + 0.0940 \times e_{BARX1-DT} + 0.1254 \times e_{LSAMP-AS1} + 0.1400 \times e_{HOXB-AS4} + 0.1560 \times e_{MNX1-AS1} + 0.1611 \times e_{LINC01385} + 0.0959 \times e_{LINC02893}$. The risk scores of the seven-lncRNAs panel were significantly associated with poor OS (HR:6.21 [3.27-11.81], $p < 0.0001$), DSS (HR:4.34 [1.83-10.26], $p = 0.0008$), and PFI (HR:3.78 [1.92-7.43], $p = 0.0001$) in TCGA cohort. Based on the median value of the risk scores, all patients in the TCGA cohort were divided into high and low risk groups. K-M survival analysis revealed that LSCC patients in the high risk group had shorter median OS (23.17 months), DSS (48.87 months), and PFI (19.23 months) than those in the low risk group (OS: 91.10 months, DSS: 213.90 months, and PFI: 213.90 months; Figures 4B, S6A, C).

Time-dependent ROC curves were drawn to assess the prognostic ability of the seven-lncRNAs risk scores. In the time frame of 1-, 3-, and 5-years, the AUC index of the seven-lncRNAs risk score for OS were 65.77%, 78.97%, and 80.76%; for DSS were 58.47%, 75.99%, and 76.55%; and for PFI were 63.20%, 73.41%, and 74.70%, respectively (Figures 4C, S6B, D). To validate the seven-lncRNAs prognostic model, the expression levels of these lncRNAs in 86 LSCC samples were determined by qPCR, then the association between seven-lncRNAs risk score and overall survival of the 86 LSCC patients was evaluated by Kaplan-Meier analysis. As expected, results further confirmed that the seven-lncRNAs model was able to predict prognosis of LSCC patients (Figure 4D). Furthermore, time-dependent ROC curves analysis showed that the AUC index of the seven-lncRNAs risk score of the 86 LSCC patients were 54.90%, 62.90%, and 69.10% in the time frame of 1-, 3-, and 5-years for OS (Figure 4E).

We also noted that LSCC patients in the low risk group had a lower mortality rate (20/55 patients, 36.36%) than those in the high risk group (30/56 patients, 53.57%; Figures 5A, B). Furthermore, the

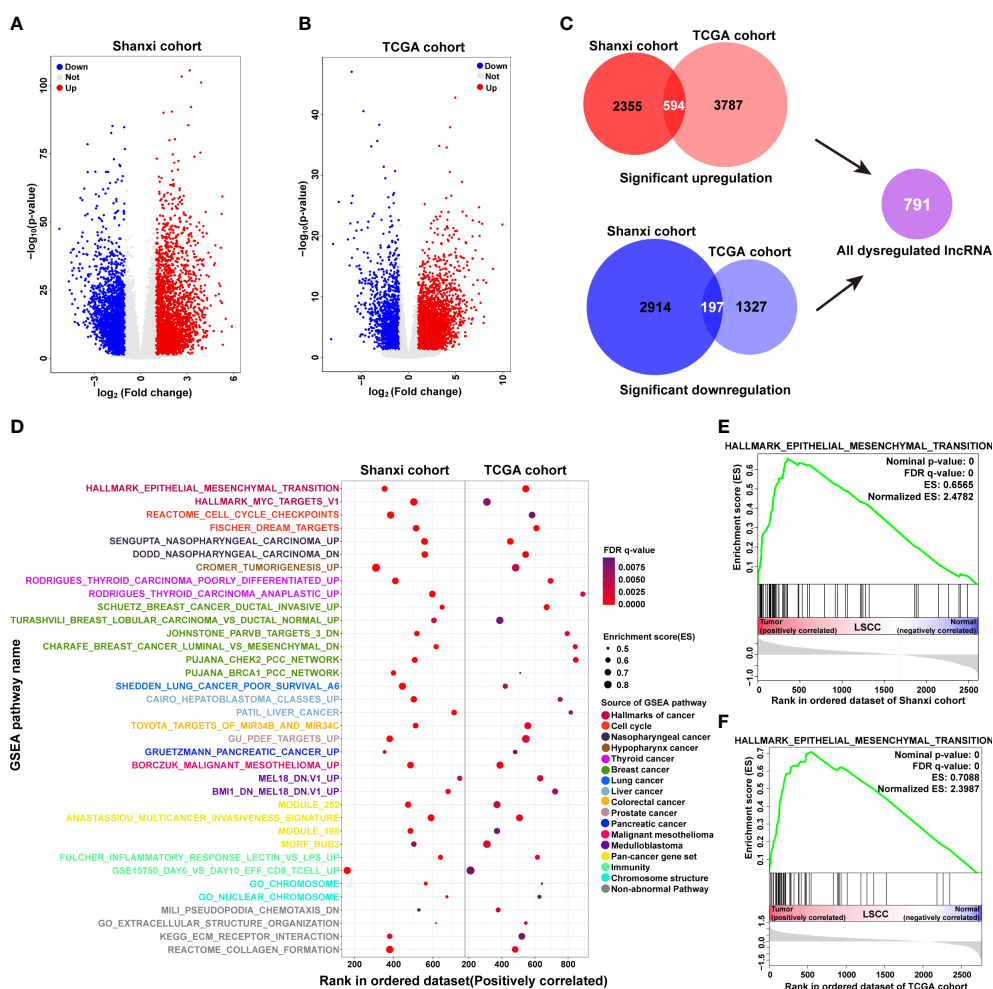


FIGURE 2 Functional annotation of significantly dysregulated lncRNAs in LSCC. (A, B) Volcano plots showing differentially expressed lncRNAs in the Shanxi (A) and TCGA (B) cohorts. (C) Analysis of the common differentially expressed lncRNAs in both Shanxi and TCGA cohorts, red: significantly upregulated lncRNAs; blue: significantly downregulated lncRNAs. (D) Functional annotation of the common differentially expressed lncRNAs in both Shanxi and TCGA cohorts by GSEA. (E, F) Enrichment plot of the EMT pathway in the Shanxi (E) and TCGA (F) cohorts.

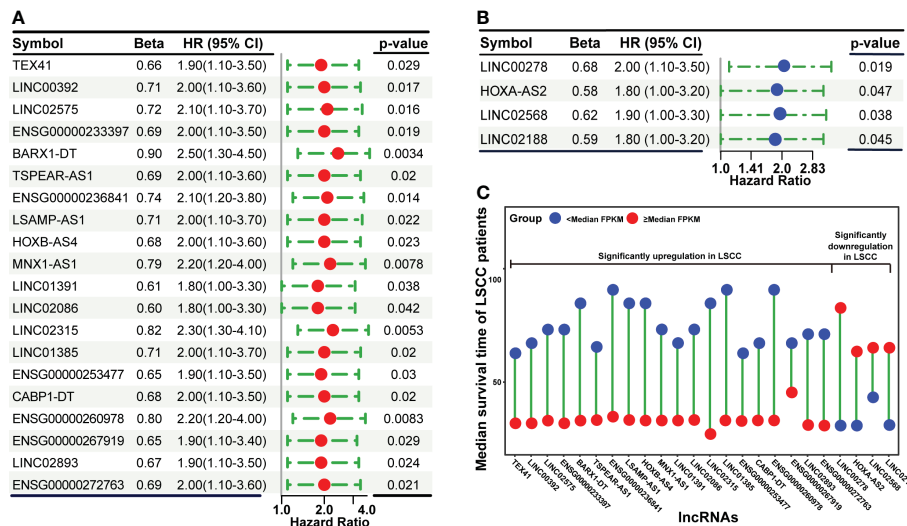


FIGURE 3 Cox proportional hazards regression analysis of significantly dysregulated lncRNAs using patients' clinical information in the TCGA dataset. **(A)** Forest plot showing the upregulated lncRNAs that are significantly associated with OS. **(B)** Forest plot showing the downregulated lncRNAs that are significantly associated with OS. **(C)** The correlation between lncRNAs expression levels and median survival time of LSCC patients.

identified seven lncRNAs had higher expression levels in patients of the high risk group than those in the low risk group (Figure 5C). Further analysis of the seven-lncRNAs data of the 86 LSCC patients showed that patients in high risk group had a higher mortality rate (13/43 patients, 30.23%) than those in the low risk group (6/43

patients, 13.95%), and patients in high risk group had higher expression levels of seven lncRNAs (Figures 5D-F).

To analyze the interconnections among seven lncRNAs, a total of 18 miRNAs was predicted based on ceRNA hypothesis (Figure S7A). LINC01385 and BARX1-DT had a common targeted miRNA

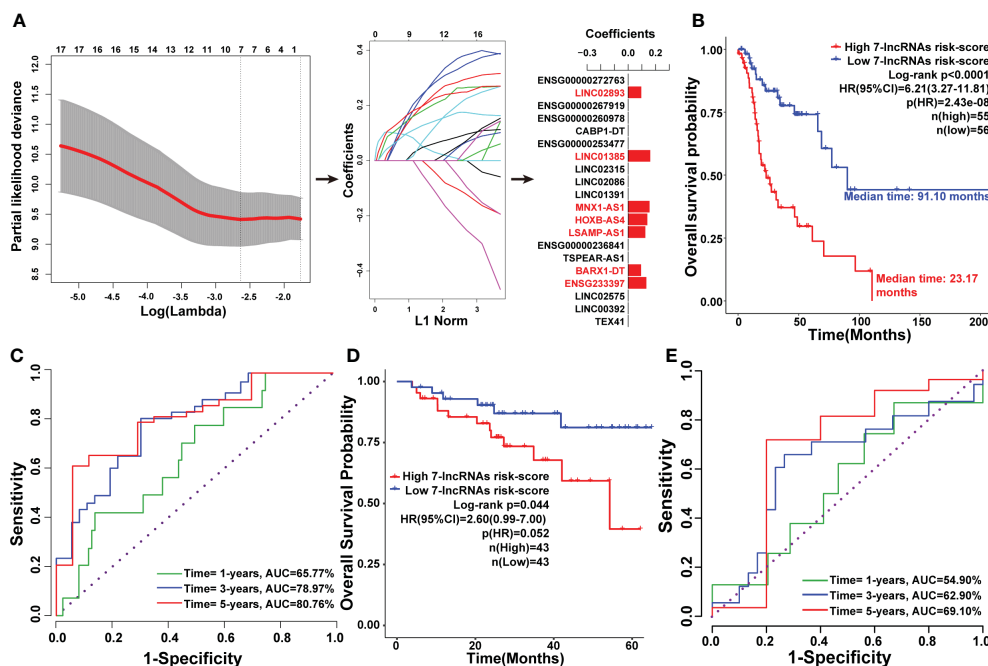


FIGURE 4 Construction of the seven-lncRNAs signature for predicting prognosis of LSCC patients. **(A)** Schematic representation of the LASSO algorithm workflow for the construction of the seven-lncRNAs signature. **(B)** K-M survival analysis showing the effect of the seven-lncRNAs signature risk score in the OS of LSCC patients in TCGA cohort. **(C)** The ROC curve for the seven-lncRNAs signature risk score in predicting the 1-, 3-, and 5-years OS of LSCC patients in TCGA cohort. **(D)** K-M survival analysis showing the efficiency of the seven-lncRNAs signature risk score in the OS of LSCC patients in 86 LSCC samples. **(E)** The ROC curve for the seven-lncRNAs signature risk score in predicting the 1-, 3-, and 5-years OS of LSCC patients in 86 LSCC samples.

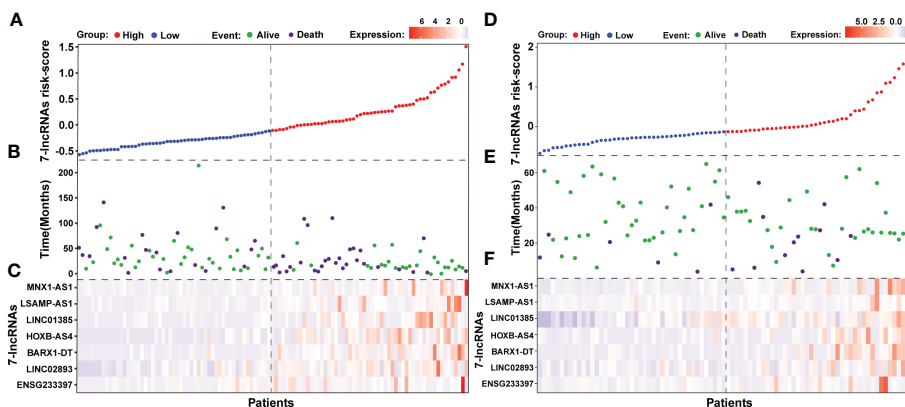


FIGURE 5 The outcome of patients and lncRNAs expression distribution between the seven-lncRNAs high and low risk groups. (A) The seven-lncRNAs signature risk scores ranked from low to high in TCGA cohort. (B) Survival status and duration of patients in TCGA cohort. (C) Heatmap showing the lncRNAs expression between the high and low risk groups in TCGA cohort. (D) The seven-lncRNAs signature risk scores ranked from low to high in 86 LSCC samples. (E) Survival status and duration of patients in 86 LSCC samples. (F) Heatmap showing the lncRNAs expression between the high and low risk groups in 86 LSCC samples.

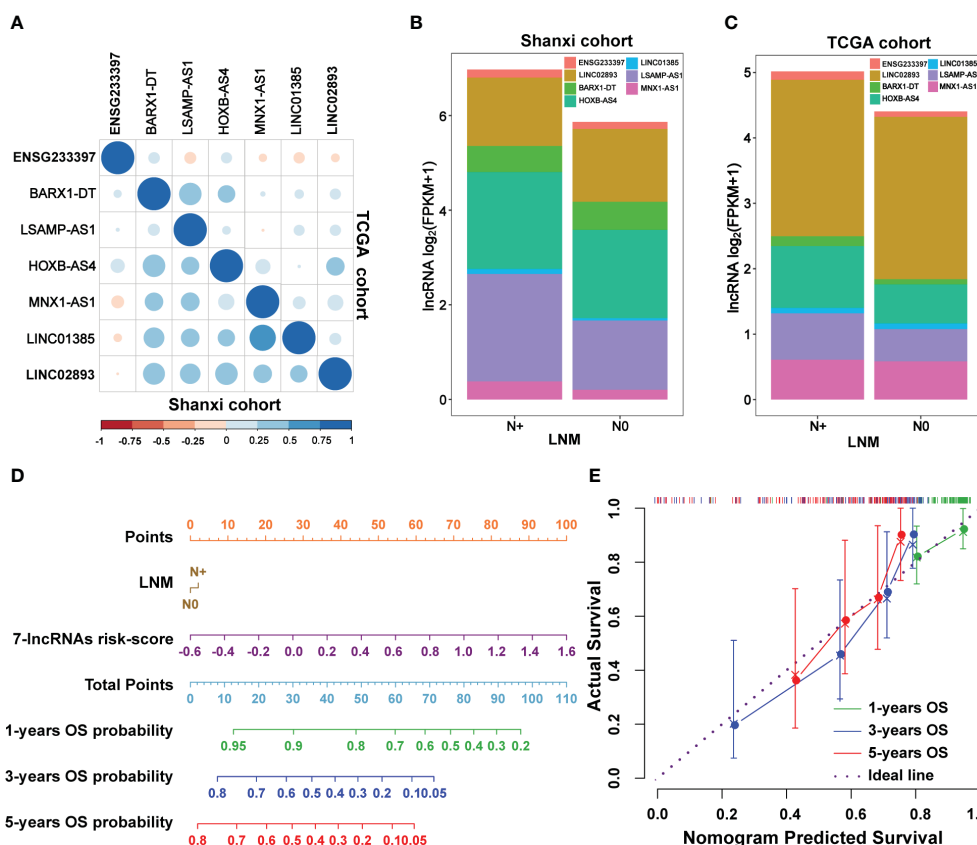


FIGURE 6 The correlation between lymph node metastasis (LNM) and the seven-lncRNAs signature. (A) The Pearson's correlation analysis showing the relationship of the seven lncRNAs with each other in the Shanxi and TCGA cohorts. (B, C) Association between the expression levels of the seven lncRNAs and lymph node metastasis in the Shanxi (B) and TCGA (C) cohorts. (D) The constructed prognostic nomogram which consists of the seven-lncRNAs signature risk score and lymph node metastasis information for predicting the 1-, 3-, and 5-years OS of LSCC patients. (E) Calibration curves of the prognostic nomogram estimating the probability of OS in 1-, 3-, and 5-years. LNM, lymph node metastasis; N0, LSCC without lymph node metastasis; N+, LSCC with lymph node metastasis.

named as miR-4739 (Figure S7B). ceRNA network analysis revealed that direct or indirect regulatory relationships were existed among these seven lncRNAs (Figure S7C). The Pearson's correlation analysis of the seven lncRNAs versus each other in the Shanxi and TCGA cohorts is seen in Figure 6A. LNM is a predominant independent factor associated with the mortality rate in LSCC (30). We found that the seven lncRNAs had relatively higher expression levels in patients with LNM than those of non-metastatic patients in both cohorts (Figures 6B, C, S8). To further improve the predictive accuracy of our model, a nomogram for OS prediction was

constructed by integrating the risk score and clinical features of LNM. As shown in Figure 6D, the upward vertical line can be respectively drawn from the line of the risk score and LNM to the line where their respective points can be calculated. Based on the sum of points of the seven-lncRNAs risk score and LNM, a downward vertical line can be drawn from the line of the total points to the line of the 1-, 3-, or 5-year OS probability to respectively calculate the OS probability. Additionally, the calibration curves for the prognostic nomogram estimating the probability of 1-, 3-, and 5-years OS performed well with the

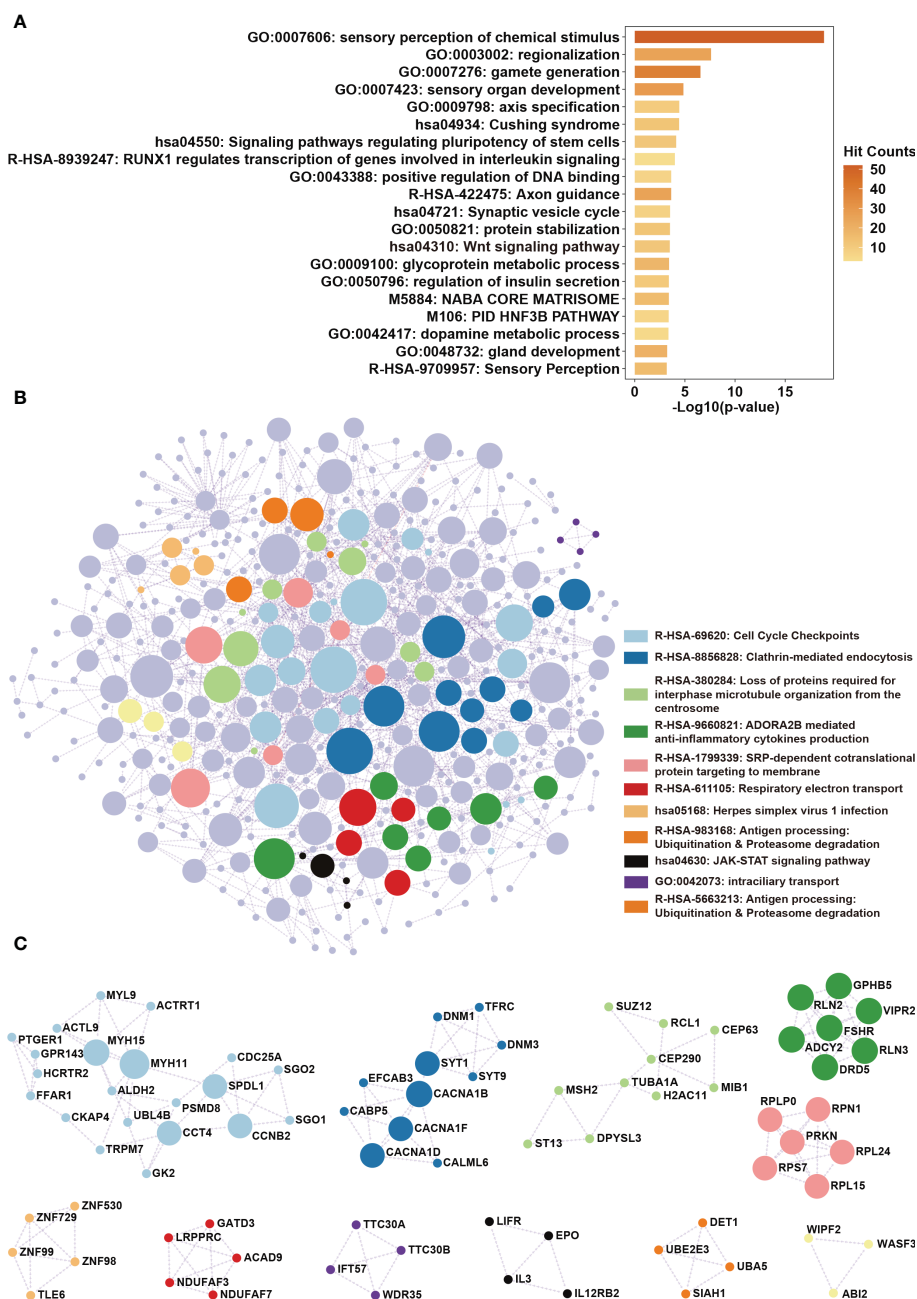


FIGURE 7 Functional annotation of the lncRNAs in the seven-lncRNAs panel. (A) Protein-coding genes whose expression levels were correlated with lncRNAs ENSG233397, BARX1-DT, LSAMP-AS1, HOXB-AS4, MNX1-AS1, LINC01385, and LINC02893 were obtained by correlation analysis. KEGG pathway and biological process enrichment analysis were performed using Metascape. (B) Protein-protein interaction enrichment analysis involving the protein products of the identified genes. (C) Protein complexes identified in protein-protein interaction enrichment analysis were highlighted.

ideal model (Figure 6E). Decision curve analysis of the prognostic nomogram for 1-, 3-, and 5-years OS risk showed that the model has a net benefit of risk stratification in the gradient prediction time (Figure S9). Collectively, these findings demonstrated that a seven-lncRNAs panel for predicting the prognosis of LSCC patients was constructed using an integrated analysis of our large-scale RNA-seq data and the TCGA data.

Knockdown of each of the seven lncRNAs inhibits the proliferation, migration, and invasion of LSCC cells

We sought to determine whether the lncRNAs are involved in regulating LSCC progression. We used the protein-coding genes whose expression levels significantly correlated with the seven lncRNAs for functional annotation through Metascape (Table S5). Results showed that the seven lncRNAs were mainly involved in the Wnt signaling pathway and pathways regulating the pluripotency of stem cells (Figure 7A). Furthermore, protein-protein interaction enrichment analysis revealed that the seven lncRNAs were also involved in cell cycle checkpoints and the JAK-STAT signaling pathway (Figures 7B, C). Since these pathways are known to contribute to cellular growth and differentiation, we hypothesized that these lncRNAs may regulate the progression of LSCC.

To investigate the functional roles of each of the seven lncRNAs in our model, we performed siRNA-mediated knockdown targeting the identified lncRNAs in LSCC cell models. Our qPCR analysis confirmed that the expression levels of the seven lncRNAs decreased significantly in the LSCC cell lines FD-LSC-1 and TU-177 after siRNAs transfection (Figure 8). The EdU staining results

showed that knocking down ENSG233397, BARX1-DT, LSAMP-AS1, HOXB-AS4, MNX1-AS1, LINC01385, and LINC02893, separately, inhibits the proliferation of LSCC cells to different degrees (Figures 9A, S10A). In addition, we found that knockdown of each of the seven lncRNAs resulted in significantly decreased migration and invasion abilities of LSCC cells (Figures 9B, C; S10B, C). Collectively, our findings suggest that the lncRNAs used in our model promote the proliferation, migration, and invasion abilities of LSCC cells *in vitro*.

Discussion

Although increasing clinical studies and advancements in treatment have been done in recent years, satisfactory therapeutic strategies and accurate prognosis predictors for LSCC have not yet been developed (31). To date, conventional cytopathology and histopathology analysis are still the sole methods for the clinical diagnosis of LSCC. Previous studies have identified several potential pathologic factors contributing to LSCC, including smoking, alcohol drinking, air pollution, HPV infection, and sex hormone receptor levels (32, 33). However, the detailed mechanism underlying tumorigenesis and progression of LSCC remains unclear. In addition, no molecular biomarkers are currently used for the diagnosis and assessment of progression as well as prognosis in LSCC (34). Therefore, the identification of molecular biomarkers to diagnose LSCC at an early stage and predict the disease progression and prognosis is urgent for clinicians and researchers.

lncRNAs have shown obvious advantages as biomarkers of human disease, particularly for the diagnosis and prognosis of cancers (7, 35): (1) The large number of lncRNAs provides a wide range of options for

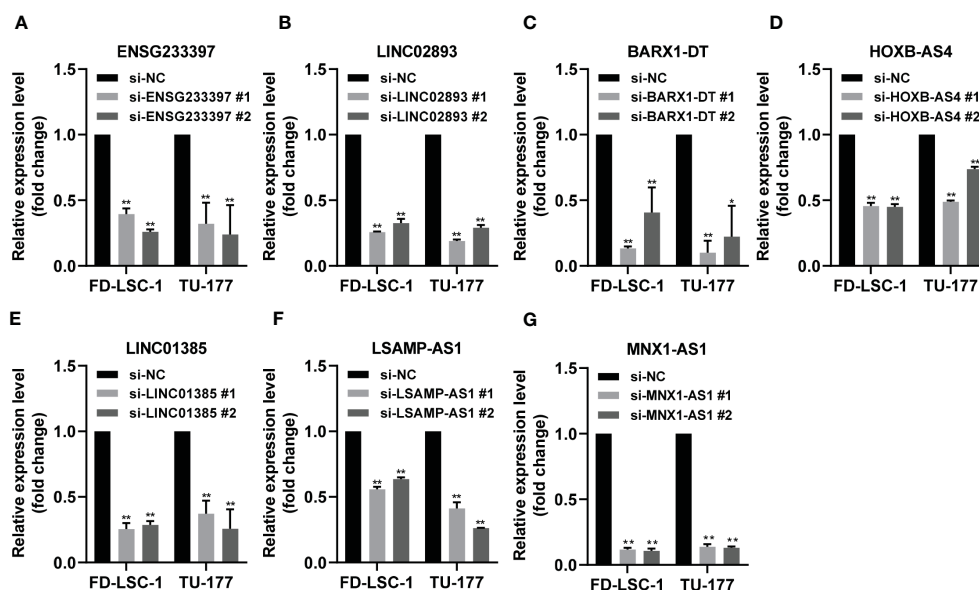


FIGURE 8

Validation of the knockdown efficiency by qPCR analysis. (A–G) FD-LSC-1 and TU-177 cells were transfected with siRNAs targeting each of the lncRNAs ENSG233397 (A), LINC02893 (B), BARX1-DT (C), HOXB-AS4 (D), LINC01385 (E), LSAMP-AS1 (F), and MNX1-AS1 (G), respectively. After 48 h of transfection, the expression levels of each of the lncRNAs were determined by qPCR analysis. All experiments were repeated three times, data are shown as mean \pm SD. ** $p < 0.01$.

finding new biomarkers; (2) lncRNA acts in various forms, which reflects the complexity of gene regulatory network in cancer; (3) lncRNA exists in various materials, such as tissue, peripheral blood, exosome, thereby providing a variety of detection and sampling methods for diagnosis; (4) lncRNA expression is tissue and spatio-temporal specific, which is of great value in diagnosis, pharmacodynamic evaluation, and prognosis evaluation. Hence, the identification of lncRNA biomarkers is of great significance for the diagnosis and assessment of the prognosis of LSCC.

Recently, several lncRNAs have been identified as potential biomarkers for the diagnosis and prognosis of LSCC. Liang et al. reported that the high expression of the lncRNA snaR was associated with the progression and poor prognosis of LSCC (36). In addition, the high expression of LINC01194 has been shown to be negatively correlated with the clinical outcome of LSCC patients (37). Moreover, the low expression of lncRNA SBF2-AS1 was correlated to lymph node metastasis, advanced clinical stage, as well as poor prognosis of LSCC (38). Despite of

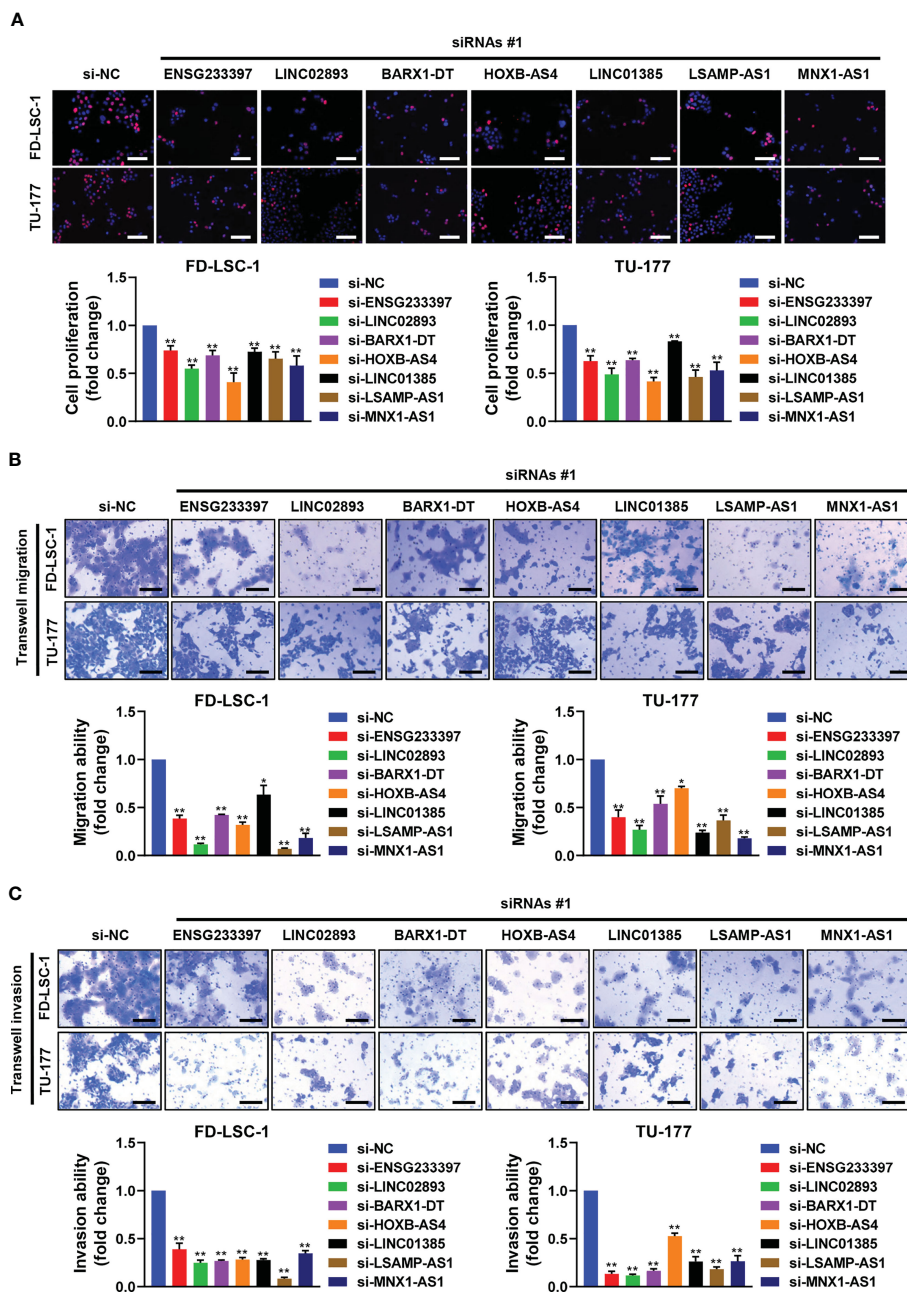


FIGURE 9 Effects of the seven lncRNAs on the cell proliferation, migration, and invasion of LSCC cells. FD-LSC-1 and TU-177 cells were transfected with siRNAs targeting the lncRNAs ENSG233397, BARX1-DT, LSAMP-AS1, HOXB-AS4, MNX1-AS1, LINC01385, and LINC02893, respectively. **(A)** Cell proliferation was assessed by EdU staining. Scale bar, 100 μ m. **(B)** Cell migration ability was assessed by trans-well migration assay. Scale bar, 200 μ m. **(C)** Cell invasion ability was assessed by trans-well invasion assay. Scale bar, 200 μ m. All experiments were repeated three times, data are shown as mean \pm SD. * $p < 0.05$, ** $p < 0.01$.

these findings, no lncRNA biomarker was used to predict the prognosis of LSCC clinically. Hence, identifying more lncRNA biomarkers with high specificity for evaluating LSCC progression and prognosis is needed. In the identification of biomarkers, large sample sizes are used to overcome substantial inter-study heterogeneity and enhance reliability (39, 40). In the current study, RNA-seq data of 107 LSCC and paired ANM tissues were integrated with the TCGA-published LSCC RNA-seq data to identify differentially expressed lncRNAs between LSCC and normal tissues. To the best of our knowledge, the sample size used in this study is much larger than that of previous studies, which makes our results more robust and reliable.

Pathway analysis revealed that dysregulated lncRNAs in LSCC were involved in cancer-related biological processes and pathways, such as epithelial to mesenchymal transition, nasopharyngeal carcinoma, cell cycle checkpoints, tumorigenesis, thyroid carcinoma poorly differentiated, and malignant mesothelioma. These findings indicate that the dysregulation of lncRNAs is crucial in regulating LSCC phenotypes. Moreover, these lncRNAs may regulate LSCC progression through the above-mentioned pathways.

Recent studies reported that multi-genes signature has a more precise predictive performance than using a single biomarker (36). We constructed a seven-lncRNAs panel (ENSG233397, BARX1-DT, LSAMP-AS1, HOXB-AS4, MNX1-AS1, LINC01385, and LINC02893) that has high specificity and sensitivity for predicting prognosis of LSCC. MNX1-AS1 is a well-known oncogenic lncRNA in multiple types of cancers such as gastric cancer (41), colorectal cancer (42), and hepatocellular carcinoma (43). Liu et al. reported that high expression of LSAMP-AS1 was associated with the poor prognosis of LSCC (44). High expression of LINC01385 was correlated with advanced clinical features and poor prognosis of nasopharyngeal carcinoma (NPC), and knockdown of LINC01385 inhibited the proliferation and invasion abilities of NPC cells (45). Moreover, upregulation of LINC02893 in non-small cell lung cancer is associated with poor prognosis (46). Based on the bioinformatic analysis results, we speculated that there are potential mutual regulatory relationships among these seven lncRNAs. On the one hand, a lot of mRNAs was regulated by shared lncRNAs, these mRNAs may affect expression levels of these lncRNAs in turn. On the other hand, some of the seven lncRNAs have common target miRNA, for example, both LINC01385 and BARX1-DT target miR-4739.

In this study, we further explored the functional roles of the seven lncRNAs used in our model. Our data revealed that the knockdown of each of the seven lncRNAs suppressed the cell proliferation, migration, and invasion abilities of LSCC cells *in vitro*. The downregulation of the seven lncRNAs contributes to the suppression of proliferation, migration, and invasion of LSCC cells, suggesting that these lncRNAs act as oncogenes in LSCC. Therefore, the seven lncRNAs may be potential targets for LSCC therapy. Further studies to uncover the molecular mechanisms underlying the activities of these lncRNAs in regulating the development of LSCC are required in the future.

In conclusion, we developed a seven-lncRNAs signature for predicting the prognosis of LSCC patients based on RNA-Seq data of more than two hundred LSCC patients from two cohorts. Risk scores and prognostic nomogram generated using the seven-lncRNAs signature performed well in evaluating the survival probability of LSCC patients. Furthermore, the lncRNAs used in our model promote proliferation, migration, and invasion of LSCC cells *in vitro*. Our findings provide a new potential multi-lncRNAs signature for predicting the prognosis of LSCC patients. More importantly, the RNA-seq dataset obtained in this study could be used as a resource of future basic and clinical cancer research.

Data availability statement

The datasets presented in this study can be found in online repositories. The names of the repository/repositories and accession number(s) can be found below: Gene Expression Omnibus, accession numbers GSE127165 and GSE130605.

Ethics statement

The studies involving human participants were reviewed and approved by the medical ethics committee of First Hospital of Shanxi Medical University. The patients/participants provided their written informed consent to participate in this study.

Author contributions

Conceptualization: YW, CA, WG. Data curation: KW, ZG, WG, YW. Formal analysis: XWZ, WG, ZZ, XX, MM, QG, DW. Funding acquisition: YW, CA, XHZ, ZZ, WG. Investigation: XWZ, WG, ZZ, XX, MM, QG, DW. Methodology: KW, ZG, WG, LX, YW. Project administration: YW, CA, XHZ, WG. Resources: YW, ZG, WG. Supervision: YW, CA, XHZ. Validation: XWZ, WG, XX, MM, QG, DW. Visualization: XWZ, WG, XX, YW. Writing - review & editing: XWZ, WG, YW, CA, XHZ. All authors contributed to the article and approved the submitted version.

Funding

This work was supported by the National Natural Science Foundation of China (No. 82073101, and 82172961), Shenzhen Science and Technology Program (RCJC20210706091950028), Guangdong Basic and Applied Basic Research Foundation (No. 2023A1515010342), Research Project Supported by Shanxi Scholarship Council of China (No. 2020165), Fund for the Scientific Activities of Selected Return Overseas Professionals in Shanxi Province (No. 20200034), Natural Science Foundation of Shanxi Province (No. 20210302124088, and 201805D211007), Shenzhen Key Medical Discipline Construction Fund (No.

SZXX039), Shenzhen Key Laboratory Foundation (No. ZDSYS20200811143757022), the Research Funds for China Central Government-guided Development of Local Science and Technology (No. 2020-165-19), the Research Project of Shanxi Province Health and Family Planning Commission (No. 2019033), the Non-profit Central Research Institute Fund of Chinese Academy of Medical Sciences (No. 2019-RC-HL-004), Beijing Hope Run Special Fund of Cancer Foundation of China (No. LC2018L06, and LC2020A19).

Conflict of interest

The authors declare that the research was conducted in the absence of any commercial or financial relationships that could be construed as a potential conflict of interest.

References

- Qi H, Chen W, Zhang C, Zheng X, Peng C, Zhao Q, et al. Epidemiological analysis of 1234 cases of laryngeal cancer in shanxi province, China. *Cancer Control* (2021) 28:10732748211041236. doi: 10.1177/10732748211041236
- Sung H, Ferlay J, Siegel RL, Laversanne M, Soerjomataram I, Jemal A, et al. Global cancer statistics 2020: GLOBOCAN estimates of incidence and mortality worldwide for 36 cancers in 185 countries. *CA Cancer J Clin* (2021) 71(3):209–49. doi: 10.3322/caac.21660
- Steuer CE, El-Deiry M, Parks JR, Higgins KA, Saba NF. An update on larynx cancer. *CA Cancer J Clin* (2017) 67(1):31–50. doi: 10.3322/caac.21386
- Gao W, Zhang Y, Luo H, Niu M, Zheng X, Hu W, et al. Targeting SKA3 suppresses the proliferation and chemoresistance of laryngeal squamous cell carcinoma via impairing PLK1-AKT axis-mediated glycolysis. *Cell Death Dis* (2020) 11(10):919. doi: 10.1038/s41419-020-03104-6
- Gao W, Guo H, Niu M, Zheng X, Zhang Y, Xue X, et al. circPARD3 drives malignant progression and chemoresistance of laryngeal squamous cell carcinoma by inhibiting autophagy through the PRKCI-Akt-mTOR pathway. *Mol Cancer* (2020) 19(1):166. doi: 10.1186/s12943-020-01279-2
- Gao W, Zhang C, Li W, Li H, Sang J, Zhao Q, et al. Promoter methylation-regulated miR-145-5p inhibits laryngeal squamous cell carcinoma progression by targeting FSCN1. *Mol Ther* (2019) 27(2):365–79. doi: 10.1016/j.ymthe.2018.09.018
- Song Q, Lv X, Ru Y, Dong J, Chang R, Wu D, et al. Circulating exosomal gastric cancer-associated long noncoding RNA1 as a noninvasive biomarker for predicting chemotherapy response and prognosis of advanced gastric cancer: a multi-cohort, multi-phase study. *EBioMedicine* (2022) 78:103971. doi: 10.1016/j.ebiom.2022.103971
- Singhi AD, Wood LD. Early detection of pancreatic cancer using DNA-based molecular approaches. *Nat Rev Gastroenterol Hepatol* (2021) 18(7):457–68. doi: 10.1038/s41575-021-00470-0
- Roy S, Kanda M, Nomura S, Zhu Z, Toiyama Y, Taketomi A, et al. Diagnostic efficacy of circular RNAs as noninvasive, liquid biopsy biomarkers for early detection of gastric cancer. *Mol Cancer* (2022) 21(1):42. doi: 10.1186/s12943-022-01527-7
- Quinn JJ, Chang HY. Unique features of long non-coding RNA biogenesis and function. *Nat Rev Genet* (2016) 17(1):47–62. doi: 10.1038/nrg.2015.10
- Hu W, Jin L, Xu A, Wang Y, Thorne RF, Zhang X, et al. GUARDIN is a p53-responsive long non-coding RNA that is essential for genomic stability. *Nat Cell Biol* (2018) 20(4):492–502. doi: 10.1038/s41556-018-0066-7
- Xiu B, Chi Y, Liu L, Chi W, Zhang Q, Chen J, et al. LINC02273 drives breast cancer metastasis by epigenetically increasing AGR2 transcription. *Mol Cancer* (2019) 18(1):187. doi: 10.1186/s12943-019-1115-y
- Gu H, Xia Y, Guo L, Wang Z, Wu S, Xu Y, et al. Long non-coding RNA MILNR1 retards colorectal cancer growth by inhibiting c-myc. *Cancer Commun (Lond)* (2020) 40(9):456–60. doi: 10.1002/cac2.12079
- Li G, Kryczek I, Nam J, Li X, Li S, Li J, et al. LIMIT is an immunogenic lncRNA in cancer immunity and immunotherapy. *Nat Cell Biol* (2021) 23(5):526–37. doi: 10.1038/s41556-021-00672-3
- Xu F, Huang M, Chen Q, Niu Y, Hu Y, Hu P, et al. LncRNA HIF1A-AS1 promotes gemcitabine resistance of pancreatic cancer by enhancing glycolysis through modulating the AKT/YB1/HIF1 α pathway. *Cancer Res* (2021) 81(22):5678–91. doi: 10.1158/0008-5472.CAN-21-0281
- Wei H, Xu Z, Chen L, Wei Q, Huang Z, Liu G, et al. Long non-coding RNA PAARH promotes hepatocellular carcinoma progression and angiogenesis via

Publisher's note

All claims expressed in this article are solely those of the authors and do not necessarily represent those of their affiliated organizations, or those of the publisher, the editors and the reviewers. Any product that may be evaluated in this article, or claim that may be made by its manufacturer, is not guaranteed or endorsed by the publisher.

Supplementary material

The Supplementary Material for this article can be found online at: <https://www.frontiersin.org/articles/10.3389/fonc.2023.1106249/full#supplementary-material>

upregulating HOTTIP and activating HIF-1 α /VEGF signaling. *Cell Death Dis* (2022) 13(2):102. doi: 10.1038/s41419-022-04505-5

17. Li Y, Jiang T, Zhou W, Li J, Li X, Wang Q, et al. Pan-cancer characterization of immune-related lncRNAs identifies potential oncogenic biomarkers. *Nat Commun* (2020) 11(1):1000. doi: 10.1038/s41467-020-14802-2

18. Wang R, Du L, Yang X, Jiang X, Duan W, Yan S, et al. Identification of long noncoding RNAs as potential novel diagnosis and prognosis biomarkers in colorectal cancer. *J Cancer Res Clin Oncol* (2016) 142(11):2291–301. doi: 10.1007/s00432-016-2238-9

19. Goyal B, Yadav SRM, Awasthee N, Gupta S, Kunnumakkara AB, Gupta SC. Diagnostic, prognostic, and therapeutic significance of long non-coding RNA MALAT1 in cancer. *Biochim Biophys Acta Rev Cancer* (2021) 1875(2):188502. doi: 10.1016/j.bbcan.2021.188502

20. Yi Q, Liu Z, Zhang K, Liu X, Wang L, Geng B, et al. The role of long non-coding RNA BCAR4 in human cancers. *Hum Cell* (2021) 34(5):1301–9. doi: 10.1007/s13577-021-00556-6

21. Garzon R, Volinia S, Papaioannou D, Mrózek Z, Bucci D, Carroll AJ, et al. Expression and prognostic impact of lncRNAs in acute myeloid leukemia. *Proc Natl Acad Sci USA* (2014) 111(52):18679–84. doi: 10.1073/pnas.1422050112

22. Yu Y, Zhang W, Li A, Chen Y, Ou Q, He Z, et al. Association of long noncoding RNA biomarkers with clinical immune subtype and prediction of immunotherapy response in patients with cancer. *JAMA Netw Open* (2020) 3(4):e202149. doi: 10.1001/jamanetworkopen.2020.2149

23. Feng L, Wang R, Lian M, Ma O, He N, Liu H, Wang H, Fang J, et al. Integrated analysis of long noncoding RNA and mRNA expression profile in advanced laryngeal squamous cell carcinoma. *PLoS One* (2016) 11(12):e0169232. doi: 10.1371/journal.pone.0169232

24. Li X, Xu F, Meng Q, Gong N, Teng Z, Xu R, et al. Long noncoding RNA DLEU2 predicts a poor prognosis and enhances malignant properties in laryngeal squamous cell carcinoma through the miR-30c-5p/PIK3CD/Akt axis. *Cell Death Dis* (2020) 11(6):472. doi: 10.1038/s41419-020-2581-2

25. Love MI, Huber W, Anders S. Moderated estimation of fold change and dispersion for RNA-seq data with DESeq2. *Genome Biol* (2014) 15(12):550. doi: 10.1186/s13059-014-0550-8

26. Wu C, Zhou L, Gong H, Du H, Tian J, Sun S, et al. Establishment and characterization of a novel HPV-negative laryngeal squamous cell carcinoma cell line, FD-LSC-1, with missense and nonsense mutations of TP53 in the DNA-binding domain. *Cancer Lett* (2014) 342(1):92–103. doi: 10.1016/j.canlet.2013.08.041

27. Wu Y, Dai F, Zhang Y, Zheng X, Li L, Zhang Y, et al. miR-1207-5p suppresses laryngeal squamous cell carcinoma progression by downregulating SKA3 and inhibiting epithelial-mesenchymal transition. *Mol Ther Oncolytics* (2021) 22:152–65. doi: 10.1016/j.omto.2021.08.001

28. Dongre A, Weinberg RA. New insights into the mechanisms of epithelial-mesenchymal transition and implications for cancer. *Nat Rev Mol Cell Biol* (2019) 20(2):69–84. doi: 10.1038/s41580-018-0080-4

29. Mittal V. Epithelial mesenchymal transition in tumor metastasis. *Annu Rev Pathol* (2018) 13:395–412. doi: 10.1146/annurev-pathol-020117-043854

30. Ho AS, Kim S, Tighiouart M, Gudino C, Mita A, Scher KS, et al. Association of quantitative metastatic lymph node burden with survival in hypopharyngeal and laryngeal cancer. *JAMA Oncol* (2018) 4(7):985–9. doi: 10.1001/jamaoncol.2017.3852

31. Cossu AM, Mosca L, Zappavigna S, Misso G, Bocchetti M, De Micco F, et al. Long non-coding RNAs as important biomarkers in laryngeal cancer and other head and neck tumours. *Int J Mol Sci* (2019) 20(14):3444. doi: 10.3390/ijms20143444
32. Qin C, Lu Y, Zhang H, Zhang Z, Xu W, Wen S, et al. Biological roles and clinical significance of estrogen and androgen receptors in head and neck cancers. *J Cancer* (2022) 13(7):2189–99. doi: 10.7150/jca.66707
33. Yang D, Shi Y, Tang Y, Yin H, Guo Y, Wen S, et al. Effect of HPV infection on the occurrence and development of laryngeal cancer: a review. *J Cancer* (2019) 10(19):4455–62. doi: 10.7150/jca.34016
34. Chana JYK, Zhenb G, Agrawal N. The role of tumor DNA as a diagnostic tool for head and neck squamous cell carcinoma. *Semin Cancer Biol* (2019) 55:1–7. doi: 10.1016/j.semcancer.2018.07.008
35. Iaccarino I, Klapper W. LncRNA as cancer biomarkers. *Methods Mol Biol* (2021) 2348:27–41. doi: 10.1007/978-1-0716-1581-2_2
36. Zhang G, Fan E, Yue G, Zhong Q, Shuai Y, Wu M, et al. Five genes as a novel signature for predicting the prognosis of patients with laryngeal cancer. *J Cell Biochem* (2020) 121(8-9):3804–13. doi: 10.1002/jcb.29535
37. Liu D, Yang H, Yuan Z, Yang X, Pei R, He H. Long noncoding RNA LINC01194 enhances the malignancy of laryngeal squamous cell carcinoma by sponging miR-655 to increase SOX18 expression. *Biochem Biophys Res Commun* (2020) 529(2):148–55. doi: 10.1016/j.bbrc.2020.05.178
38. Li Y, Tang B, Lyu K, Yue H, Wei F, Xu Y, et al. Low expression of lncRNA SBF2-AS1 regulates the miR-302b-3p/TGFBR2 axis, promoting metastasis in laryngeal cancer. *Mol Carcinog* (2022) 61(1):45–58. doi: 10.1002/mc.23358
39. Shen S, Wang G, Zhang R, Zhao Y, Yu H, Wei Y, et al. Development and validation of an immune gene-set based prognostic signature in ovarian cancer. *EBioMedicine* (2019) 40:318–26. doi: 10.1016/j.ebiom.2018.12.054
40. Hu X, Bao M, Huang J, Zhou L, Zheng S. Corrigendum: identification and validation of novel biomarkers for diagnosis and prognosis of hepatocellular carcinoma. *Front Oncol* (2020) 10:617539. doi: 10.3389/fonc.2020.617539
41. Shuai Y, Ma Z, Liu W, Yu T, Yan C, Jiang H, et al. TEAD4 modulated lncRNA MNX1-AS1 contributes to gastric cancer progression partly through suppressing BTG2 and activating BCL2. *Mol Cancer* (2020) 19(1):6. doi: 10.1186/s12943-019-1104-1
42. Wu Q, Luo X, Liu J, Lu Y, Wang Y, Qi J, et al. MYC-activated lncRNA MNX1-AS1 promotes the progression of colorectal cancer by stabilizing YB1. *Cancer Res* (2021) 81(10):2636–50. doi: 10.1158/0008-5472.CAN-20-3747
43. Ji D, Wang Y, Sun B, Yang J, Luo X. Long non-coding RNA MNX1-AS1 promotes hepatocellular carcinoma proliferation and invasion through targeting miR-218-5p/COMMD8 axis. *Biochem Biophys Res Commun* (2019) 513(3):669–74. doi: 10.1016/j.bbrc.2019.04.012
44. Liu Y, Ye F. Construction and integrated analysis of crosstalking ceRNAs networks in laryngeal squamous cell carcinoma. *PeerJ* (2019) 7:e7380. doi: 10.7717/peerj.7380
45. Li L, Zhang F. Novel long noncoding RNA LINC01385 promotes nasopharyngeal carcinoma proliferation via the miR-140-3p/Twist1 signaling pathway. *Cell Cycle* (2020) 19(11):1352–62. doi: 10.1080/15384101.2020.1750133
46. Fan Y, Zhou Y, Li X, Lou M, Gao Z, Tong J, et al. Long non-coding RNA AL513318.2 as ceRNA binding to hsa-miR-26a-5p upregulates SLC6A8 expression and predicts poor prognosis in non-small lung cancer. *Front Oncol* (2022) 12:781903. doi: 10.3389/fonc.2022.781903